ELSEVIER

General Review

Drag Forces after Thoracic Endovascular Aortic Repair. General Review of the Literature

Q1 *Maurizio Domanin,[1,2] Daniele Bissacco,[2] Rodrigo M. Romarowsky,[3] Michele Conti,[3] Ferdinando Auricchio,[3] Marco Ferraresi,[4] and Santi Trimarchi,[1,2] Milan, Italy; Pavia, Italy*

Background: Despite the great evolution of endograft devices for thoracic endovascular aortic repair (TEVAR), threatening related complication such as graft migration and endoleaks still occur during follow up. The Drag Forces (DF), that is the displacement forces that play a role in graft migration and endoleaks caused by the blood flow against the thoracic graft, can be studied by means of Computational Fluid Dynamics (CFD).

Method: A general review of papers found in current literature was performed. CFD studies available on the topic of thoracic aortic diseases and DF were analyzed. All anatomic, hemodynamics or graft related factors which could have an impact on DF were reported.

Results: Different factors deeply influence DF magnitude in the different site of the Ishimaru's zones classification: angulation, tortuosity and length of the landing zone, graft diameter, length and deployment position, blood pressure, pulse waveform, blood viscosity and patient heart rate have been related to the magnitude of DF. Moreover, also the three-dimensional orientation of DF is emerging as a fundamental issue from CFD studies. DF can be divided in sideways and upward components. The former, even of higher magnitude in zone 0, maintain always an orthogonal orientation and does not change in any type of aortic arch; the latter result strictly related to the anatomic complexity of the aortic arch with values up to four times higher in zone 3.

Conclusion: Different DF magnitude and orientation could explain how TEVAR have higher rate of migration and endoleaks when we face with more complex aortic anatomies. All these aspects should be foreseen during the planning of TEVAR procedure. In this field, collaboration between physicians and engineers is crucial, as both parts have a primary role in understanding and describing hidden aspects involved in TEVAR procedures.

INTRODUCTION

Currently, thoracic endovascular aortic repair (TEVAR) is widely being used for the treatment of thoracic aortic diseases. Compared to open aortic surgery, the treatment of thoracic aortic aneurysms (TAAs), acute and chronic dissections, penetrating aortic ulcers, intramural hematomas, and/or traumatic aortic injuries, endovascular

Funding: None.

Conflict of Interest: The authors have no personal, financial, or institutional interest in any of the drugs, materials, or devices described in this article.

Congress presentation: *Presented at 11th European Symposium on Vascular Biomaterials (ESVB 2019), Strasbourg October 17-19th, 2019.*

[1]*Department of Health and Community Sciences, University of Milan, Milan, Italy*

[2]*Fondazione IRCCS Ca' Grande Ospedale Maggiore Policlinico Milano, Milan, Italy*

[3]*Department of Civil Engineering and Architecture, University of Pavia, Pavia, Italy*

[4]*Teaching School of Vascular Surgery, Vascular Surgery Resident Program University of Milan, Italy*

Correspondence to. Santi Trimarchi, MD, PhD, Department of Health and Community Sciences, University of Milan, Unit of Vascular Surgery, Fondazione IRCCS Ca' Granda Ospedale Maggiore Policlinico, Via F. Sforza 35, 20122 Milano, Italy.; E-mail: santi.trimarchi@unimi.it

Ann Vasc Surg 2021; 000: 1–10
https://doi.org/10.1016/j.avsg.2021.02.042

Manuscript received: December 2, 2020; manuscript revised: February 16, 2021; manuscript accepted: February 22, 2021; published online: xxx

Table I. Type I/III Endoleaks and stent graft migration rate after TEVAR

Year	Authors	Patients	Pathologies	Endoleaks	Migration rate
2006	Parmer et al	105	TAA	Type I 11.0% (6 ys) Type III 1.5% (6 ys)	
2008	Makaroun et al	140	TAA	Type I 10.5% (5 ys)	
2008	Morales et al	160	TAA and aortic dissection	Type I 6.25% (6 ys) Type III 1.8% (6 ys)	
2018	Geisbusch et al	123	Acute aortic syndromes and TAA	Type I/III 44.0%	7.0% (6 ys) 13.9% (5 ys)

repair is less invasive and the recovery time of patients is shorter.[1–3] However, stent-graft related complications still occur during the follow up period. Endograft migration and endoleaks are the most common and threatening complications, and their findings create concerns among vascular surgeons because of their role as a precursor of reintervention. The definition of stent graft migration is "a shift of > 10 mm relative to a primary anatomic landmark or any displacement that led to symptoms or required therapy during follow-up".[4] Geisbusch et al. recently reported in a series of 123 TEVAR for Acute Aortic Syndromes and TAAs a migration rate of 7.3% in a median follow up of 3 years. Freedom from migration declines progressively over time, reaching 13.9% after 5 years of follow up.[5] Endograft migration after TEVAR can result in a sealing zone failure that may lead to the development of type I endoleaks and thereby, an increased risk of delayed aortic rupture. Similarly, an increased rupture risk may occur when the migration happens at the junctional and overlapping site of two stent-graft sections, determining a type III endoleak. Parmer et al. observed during a follow-up period of 17.3 ± 14.7 months in 105 patients with two different devices, an 11% incidence for Type I endoleak and 1.5% for type III endoleak.[6] Makaroun et al. in a pivotal trial utilizing the Gore-TAG (W.L. Gore and Associates, Flagstaff, AZ – USA) endoprosthesis reported mainly type I endoleaks in 10.6% patients during 5 years follow-up.[7] Morales et al observed 6.25% type I and 1.8% type III endoleaks in 160 patients treated with Zenith (Cook Inc, Bloomington, IN) thoracic devices. [8] Geisbüsch et al. observed Type I or Type III endoleaks in 44% (4/9) of the cases with stent-graft migration mainly located in the overlapping zone or at the distal landing zone (Fig. 1 and Table I).[5]

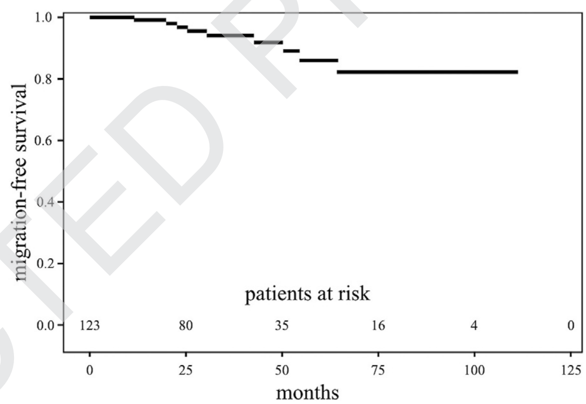

Fig. 1. Kaplan Meier curve of stent graft migration-free survival after thoracic endovascular repair at 10 years (This picture was previously published in Geisbüsch P, Skrypnik D, Ante M, Trojan M, Bruckner T, Rengier F, Böckler D. Endograft migration after thoracic endovascular aortic repair. J Vasc Surg 2018;69:1387-94.)[5]

Reintervention rate has been reported to be 38-72% for acute dissection, 13–41% for chronic dissections and 8–22% for TAA at 3 years.[9–15] In particular, TAAs are more frequently associated with proximal or distal endograft extension for Type I endoleak or supplemental stent placement for Type III endoleak compared to aortic dissections.[16] The treatment for penetrating aortic ulcers, intramural hematomas and aortic transaction requires a shorter aortic coverage, therefore they have a reduced incidence of secondary interventions.[5,17] Aortic complex anatomy presenting with a short and tortuous landing zone can be associated with challenging TEVAR procedures. It is also important to know that, after implanting a stent graft, the aortic wall changes as the stent graft is less compliant than normal aortic tissue. Such situation may come with a new hemodynamic stress forces that impact differently.[18–19] Thanks to the development of high-performance computing and to the advancements of clinical imaging, Computational Fluid Dynamic (CFD) allows to simulate challenging and clinically relevant problems, which cannot be measurable by conventional ultrasound or radiological technologies, into numerical simulations useful to improve the clinical decision making.

For a successful translational process that allow to transfer the information obtained by CFD modelling from the bench to the bedside, CFD output should be tuned to specific clinical scenarios and surgical needs. Vascular practical results as an ideal field of application for CFD analysis, which can be used both for the analysis of native vascular pathologies [20–21] or to improve surgical procedures in different localizations of vascular pathologies.[22–24] CFD modeling techniques have demonstrated also their usefulness to analyze the direction and magnitude of drag forces (DF) that act on the aortic wall.

The objective of this state-of-the-art review is to analyze the role of hemodynamic DF throughout the Descending Thoracic Aorta (DTA) in patients with thoracic aortic diseasess and how CFD could help to obtain successful and durable results after endovascular interventions.

METHODS

Articles search method and presentation were performed according to the Scale for the Assessment of Narrative Review Articles (SANRA), a six-items scale developed for the quality assessment of narrative review articles.[25] Despite SANRA was usually used during the peer-review process, Authors tried to obtain the maximum score possible (12 points) in order to improving the quality of manuscript. For this purpose, Authors used SANRA during the article pre-writing planning, adopting recommendations provided by instructions document.[26] Furthermore, recommendations from Green and collaborators were also adopted.[27]

MEDLINE (PubMed), Embase and The Cochrane Library were interrogated between May 31, 2000 and May 31, 2019 (20 years), among articles in English language. Only papers regarding description, analysis and clinical implication of DF were included. No exclusion criteria were adopted among articles screened for the main topic. Results analysis was presented as a state-of-the-art review, describing methods used to obtain CFD images, their interpretation, implications and future perspectives.

Keywords were selected using medical subject headings for MEDLINE and The Cochrane Library and the EMTREE terms for Embase. Keywords as “drag forces”, “aortic hemodynamic”, “TEVAR”, “computed-base simulation”, “complications” and “follow-up studies” were combined to obtain the first publications cluster. To connect terms with each other the Boolean operators “AND” and “OR” were used. The peer-review journals Annals of Vascular Surgery, Annals of Thoracic surgery, Journal of Cardiac Surgery, Journal of Cardiovascular Surgery, European Journal of Vascular And Endovascular Surgery, Journal of Endovascular Therapy, European Journal of Cardio-thoracic Surgery, Journal of Vascular Surgery, and Circulation were interrogated on June 6, 2019 in order to find articles published “online first” and not yet indexed on scientific online database. The same process was performed for bioengineering journals, as Nature Biomedical Engineering, Annual Review of Biomedical Engineering, IEEE Transactions on Biomedical Engineering, Annals of Biomedical Engineering, Journal of Biomedical Engineering, Medical Engineering & Physics,

Journal of Biomechanics and Biomechanics and Modeling in Mechanobiology. All titles and abstracts of potentially useful articles were selected. References of all identified relevant studies were used to perform a recursive search of the literature. Metalib (Università degli Studi di Milano, Milan, Italy), SBBL (Lombard Biomedical Librarian System) and personal journal subscription were used to obtain full text articles in case of eligible titles and abstracts.

RESULTS

The non-systematic research returned several clinical and experimental articles on DF description and analysis in TEVAR, presented below. Furthermore, we defined how DFs are obtained in our experimental practice.

DISCUSSION

CFD Analysis of DFs: How to Standardize Material and Methods

The steps to obtain high quality CFD analysis are now well standardized and can be summarized in the following five steps:

1) collection of radiological imaging data set;
2) segmentation of radiological imaging;
3) geometric model construction;
4) computational simulation with reliable boundary conditions;
5) post processing and statistical analysis (Fig. 2).

CFD analysis can be performed with many different tools and libraries available as commercial or open-source software, although they often require customization for research purposes.

The starting point to perform CFD analysis is the availability of thin cut scans (possibly not

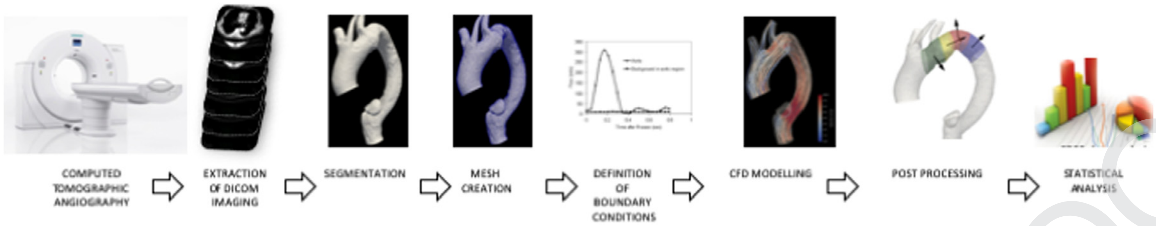

Fig. 2. Workflow to set up Computational Fluid Dynamic (CFD) modelling in thoracic aortic pathologies.

greater than 1.0 mm) obtained from Computed Tomography Angiography (CTA) or Magnetic Resonance Angiography of patients with aortic pathologies and then saved in the DICOM (.dcm) file format.

The steps to obtain high quality CFD analysis are now well standardized and can be summarized in the following five steps:

1) collection of radiological imaging data set;
2) segmentation of radiological imaging;
3) geometric model construction;
4) computational simulation with reliable boundary conditions;
5) post processing and statistical analysis (Fig. 2).

The starting-point to perform CFD analysis is the availability of thin cut slices (1.0 mm or 1.5 mm) CTA scans of patients with aortic pathologies saved in the DICOM (.dcm) file format.

Then, CFD is solved by discretizing the geometry into small element volumes formed through grid or mesh generation using various approaches, and enforcing physical laws in each single element volume. In particular, hemodynamics problems are approached computing the behavior of blood flows by solving the Navier-Stokes equations in a three-dimensional (3D) model of the region of interest (ROI). As ROI of the aortic arch, Thanks to the development of high-performance computing and to the advancements of clinical imaging, today CFD allows to simulate challenging and clinically relevant problems into numerical simulations, useful to improve the clinical decision making tool. The aorta between the valve annulus to the diaphragm, including the proximal tract of brachiocephalic trunk, left common carotid artery, and left subclavian artery is considered. The ROI is extracted from CTA scans using the open source library Vascular Modelling ToolKit (http://www.vmtk.org/).[28] The final 3D model is then exported in stereolithographic format, and artificially extended by inserting cylindrical regions, called flow extensions, at the boundary sections.[29] Such fictitious domain extensions are then removed during the post-processing analysis. This approach aimed to reduce the impact of modelling choices and uncertainties in the boundary conditions on the numerical results[30] Accordingly, by means of VMTK, a 3D aortic model is discretized to generate a computational mesh suitable for CFD analysis. Number of tetrahedral elements are based on a grid convergence analysis that showed that further mesh refining would have produced a difference of less than 1% in the computed DF. Usually the number of tetrahedrons used for aortic CFD is between 1 to 2 million elements.

Realistic boundary conditions at the inlet(s) and outlet(s) are mandatory for achieving high fidelity and accurate CFD analysis. Boundary conditions can be set using flow waveform assumed from scientific literature or using patient specific data taken from pre-operative Doppler ultrasound or intraoperative invasive measures. Blood is considered as an ideal Newtonian, homogeneous, and incompressible fluid, so that the Navier-Stokes equations are used for its mathematical description. Blood viscosity is set equal to 0.035 Poise, density equal to 1.0 g/cm3, and time step equal to 0.001 s. Given the small magnitude of the physiologically observed displacements and the fact that flow impingement patterns are not expected to critically depend on perturbations of the boundary, rigid walls are adopted.[31] The simulated cardiac cycle lasted 1 s and each computational analysis is run for six heartbeats, to ensure the convergence of velocity and pressure fields.[32] All the CFD analyses are performed using the open source parallel finite element solver based on the academic software LifeV (https://lifev.org), tailored to blood flow applications.[33]

Finally, the CFD modeling consists of the simulation of blood velocity, pressure, and wall shear stress (WSS), on each tetrahedrical element of the aortic 3D mesh over the cardiac cycle.[34] The results of the simulations are post-processed using Python script and Paraview software v4.4 (Kitware Inc., France) to isolate the aortic wall in each landing zone for each case. DF are then calculated by integrating wall pressure and WSS at systolic peak along the aortic wall. The contribution of WSS to the total DF is several orders of magnitude lesser than pressure and therefore the impact of blood viscosity is insignificant.[35] Then, magnitude and direction of the DF for each Ishimaru's landing zone are calculated.[36] A normalized DF value, defined as equivalent surface traction (EST), is calculated by dividing the DF magnitude by the surface area of the corresponding proximal landing zone. Because the surface areas of the proximal landing zones are different across the aortic arch, EST is proposed to evaluate the impact of the geometrical differences only.

At the end of the process, data are statistically analyzed. We use SPSS Statistics v.24 (SPSS Inc., Chicago, IL, USA) and post-hoc comparisons are made with the Least Significant Difference test. Continuous data are reported as the mean value with 95% CI within parentheses and statistical significance is assumed at $P < 0.05$.

DFs and Aortic Geometries: Literature Findings

DFs, in the case of TEVAR, are the resistance forces caused by the motion of the fluid (i.e., blood flow) against the body of the graft. Several studies have been performed to investigate the inner hemodynamic forces acting inside the aorta with respect of its geometry. Indeed, curvature or tortuosity affect the magnitude and direction of the DFs. With aging, as elastin fibers in the aortic wall deteriorate, DTA becomes larger, longer and more tortuous. All these features are even more common for pathological aorta and can create problems for stent graft mechanical stability and concerns of migration. Altnji et al. performed numerical simulations in a single case of TAA using finite element analysis and found attachment site length and endograft oversizing as the most important factors determining the risk of endograft migration. More specifically, with neck angulation of 60° and variable oversizing from 15% to 20%, their simulations showed endograft migration when the sealing length was 15 mm, while a sealing length of 18.5 mm resulted adequate to avoid graft migration.[37] Figueroa et al., observed that the magnitude of DF increases with increasing endografts diameter and length.[38] Prasad et al. in a single modeling study founded that DF is predominantly directed sideways in the abdominal aorta,[39] while it is directed upwards in the proximal thoracic aorta.[40] Krsmanovic et al. found that in worst-case clinical scenarios, the magnitude of the DFs exceeds the forces that an endograft is able to withstand for preventing migration.[41] These worst-case scenarios include high angulation in the landing zone, and greater diameter of the endograft. Figueroa and coworkers observed that thoracic aortic curvature is very large, and blood flow changes from the cranial direction in the ascending aorta to the caudal direction in the DTA. They also showed that an increased angulation of the aortic arch resulted in higher DFs in the proximal landing zones of the aortic arch. Nakatamari and collaborators reported greater rates of Type Ia endoleak when the curvature of the aortic arch was wider, Type Ib endoleak when the thoracoabdominal junction curvature was larger and Type III endoleak when the greater curvature was located in the midportion of the descending aorta.[42] The association between tortuosity of the thoracic aorta and outcomes of TEVAR was assessed by Chen and collaborators.[43] They analyzed 77 patients according to tortuosity index (TI) calculated by dividing the curved length by the straight distance along a centered line that was measured from 2.5 cm proximal to the proximal neck up to 2.5 cm distal to the distal neck of the thoracic aorta. Measures were obtained by computed tomographic angiography and were independently analyzed by two radiologists. The patients were divided in Low tortuosity (TI $<$ 1.29) and High tortuosity (TI $>$ 1.29) groups. The latter group had higher rates of endoleaks and worst clinical outcomes in terms of mortality at 5 years. Belvroy and collaborators, in a preliminary report, analyzing by means of CFD simulations aortic tortuosity in patients with a descending thoracic aortic aneurysm observed that higher DFs in the DTA are associated with a higher degree of tortuosity. These migration forces look to be increased in those aortic sections which present with higher tortuosity, in a sideway direction, namely lower, as noted in Figure 3A and B than in Figure 3C.[44] In the DTA, high tortuosity angle ($>$ 60°) could be associated with increased risk of stent-graft related complications, as the DF magnitudes lie within the range of pullout forces, as described by Rahmani et al.[45] Other factors that could influence the magnitude of DFs appear to be the deployment position of the endograft closer to the proximal arch,[46] blood pressure and pulse waveform[47], blood viscosity and patient heart rate.[48]

Trying to Forecast Future Graft Behavior According to the Aortic Anatomy

Currently, pre-operative planning for TEVAR of the arch is based on Ishimaru' s map which does not take into account angulation and tortuosity of the landing zone, factors that are associated

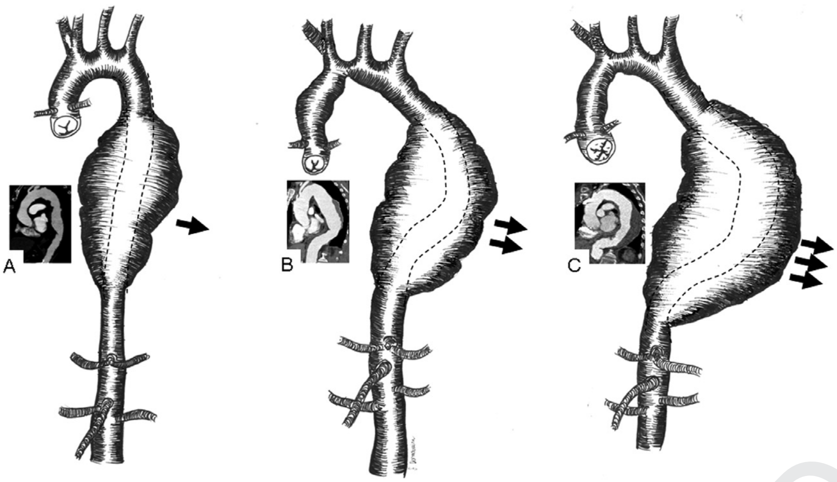

Fig. 3. Orientation of drag forces (DFs) respect of DTA tortuosity. DF result lower when the tortuosity angle is flat while DF result increased in case of higher tortuosity angle.

with higher rates of endograft failure.[44,49,50] It has been proposed to modify the classical Ishimaru's classification scheme of landing zones merging it together with the Aortic Arch Classification usually used for identification of difficulties in carotid stenting (Fig. 4).[51]

This new classification, called Modified Arch Landing Areas Nomenclature,[21] allows to predict hostile landing zones for TEVAR, as type II and type III aortic arches resulted associated with greater angulation, especially in aortic landing zones 2 and 3. The same Authors, in their attempt to improve the predictive value of the previously described geometric patterns, then reported an analysis of 15 healthy aortas selected on the basis of the three groups of Aortic Arch Classification. By means of CFD modelling, the values of the pulsatile DF with respect of the Ishimaru's proximal landing zones were obtained, analyzing also the 3D orientation of the DF acting inside the thoracic aorta.[22] Regardless of the type of arch, in Zone 0 DF magnitude resulted with the highest values ($P < 0.001$). On the contrary, comparison between types of arch, showed that DF magnitude resulted significantly different in Zone 3 ($P = 0.007$), with 3/II and 3/III significantly greater values than 3/I ($P = 0.004$ and $P = 0.008$, respectively). Furthermore, DFs magnitude in 3/III was measured almost twofold greater than in 2/III ($P = 0.033$), as also in 3/II compared with 2/II ($P = 0.032$). Regarding DFs orientation, they observed that the sideways component of DFs did not change between proximal landing zones 1–3 in any type of arch. On the opposite, the greater changes in DFs magnitude observed in 3/II and 3/III were related to the upward component that resulted four times greater in 3/II respect of 2/II ($P < 0.001$), and five times greater in 3/III respect of 2/III ($P < 0.001$) while in type I arch the upward component did not differ through proximal landing zones 1-3 (Fig. 5). DFs in Zone 0, notwithstanding their higher magnitude, resulted to have an orientation orthogonal to the longitudinal axis of the aorta. This fact could explain how TEVAR in this zone presents lesser rate of migration and endoleaks compared to other apparently quieter aortic zones. [52] Comparison of EST between the different types of arch did not show change across proximal landing zones within type I ($P = 0.297$) and type II arches ($P = 0.054$), whereas EST increased towards more distal proximal landing zones within type III ($P = 0.019$). Between adjacent landing areas, EST was calculated greater in 3/III than in 2/III ($P = 0.016$), and in 3/II than in 2/ II ($P = 0.016$). Finally, EST resulted significantly different in Zone 3 ($P = 0.009$), with that in 3/II and in 3/III being twofold greater than in 3/I ($P = 0.008$ and $P = 0.006$).

Although data were obtained from the analysis performed in healthy patients, this study has put the spotlight on DFs' distribution between different proximal landing zones in the aortic arch used for TEVAR. Moreover, this analysis has tried to overcome studies performed on aortic morphology and sizing based just on observation of radiological imaging.

Future Perspectives

If the true meaning of translational research in surgery is to transfer the process of applying knowledge from basic science to techniques that

Please cite this article as: Domanin *et al.*, Annals of Vascular Surgery(2021), https://doi.org/10.1016/j.avsg.2021.02.042

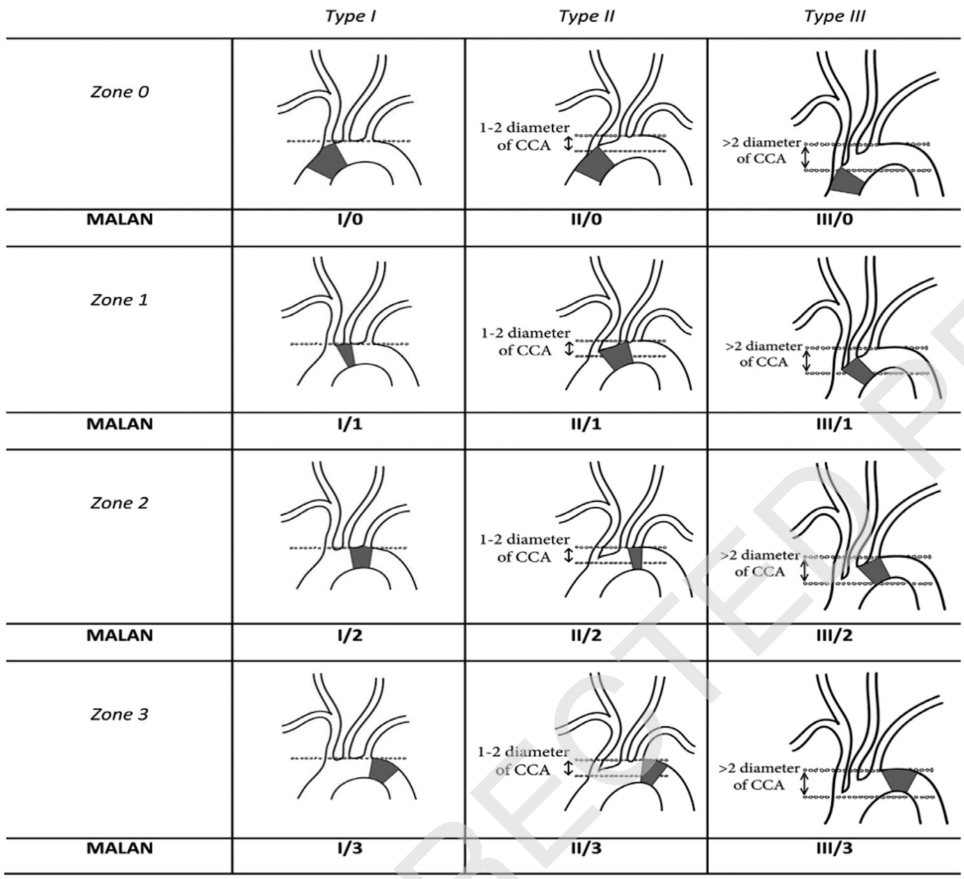

Fig. 4. The Modified Arch Landing Areas Nomenclature (MALAN) which consider the Ishimaru's Aortic Arch Map of the proximal landing zones and the Types of arch according to the Aortic Arch Classification (This picture was previously published in Marrocco-Trischitta MM,de Beaufort HW, Secchi F, van Bakel TM, Ranucci M, van Herwaarden JA, et al. A geometrical reappraisal of proximal landing zones for thoracic endovascular aortic repair according to aortic arch types. J Vasc Surg 2017;65:1584-90.)[21]

address critical operative needs, today our aim is the application of the analytical information on DFs obtained by CFD in the surgical practice.

We have learned that DFs vectors changes from proximal to distal and both the magnitude and the direction could be significantly modified by aortic geometries. In this way we should consider all these factors to prevent long term stent-graft migration and related complications when planning TEVAR. Prospective work will assess how preoperative CFD analysis on EST acting on the aortic arch and DTA wall can be applied.

As consequence, we have started to apply clinically this knowledge in some specific settings. As example we report a rather complex case of an 83 years old man with acute aortic type B dissection extended from the left subclavian artery to the celiac trunk, without any sign of malperfusion, but with a suprarenal aortic pseudoaneurysm. The proximal entry tear was placed at the supravisceral aorta with a retrograde dissection extended up to the origin of left subclavian artery (Fig. 6A). The patient was previously submitted to open aortic repair for AAA, to endovascular aortic repair for proximal anastomotic aneurysm and then to femoro-femoral crossover bypass graft for left limb occlusion. Preoperative CFD analysis, conducted for EST evaluation, showed high values in zone 3, low in zone 4a and even lower in zone 4b (Fig. 6B). After fifteen days of medical antihypertensive therapy we decided to choose according to the preoperative CFD, as landing the zone 4b considering the lower EST estimated in this location and the consequent theoretical reduced risk of late graft displacement. Thoracic endograft was deployed distal to the left subclavian artery just up the celiac trunk, excluding the entry tear. Immediate post-operative and six months follow up CTA confirmed the validity of such decision (Fig. 6C, D). No complications were observed after procedure and during initial

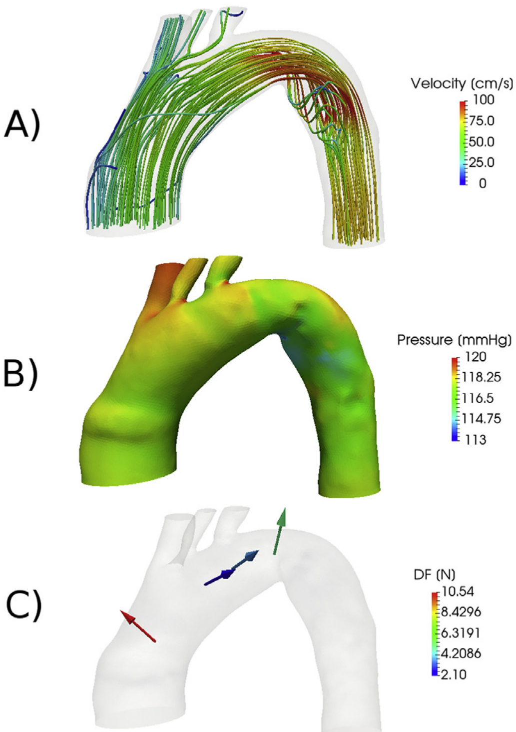

Fig. 5. Representation of the simulation results at systolic peak. The case of a Type III arch is reported. (A) Streamlines of the blood flow, (B) pressure, and (C) displacement forces for each zone. (This picture was previously published in Marrocco-Trischitta MM, van Bakel TM, Romarowski RM, de Beaufort HW, Conti M, van Herwaarden JA, et al. The Modified Arch Landing Areas Nomenclature (MALAN) Improves Prediction of Stent Graft Drag forces: Proof of Concept by Computational Fluid Dynamics Modelling. Eur J Vasc Endovasc Surg. 2018;55:584–92.)[22]

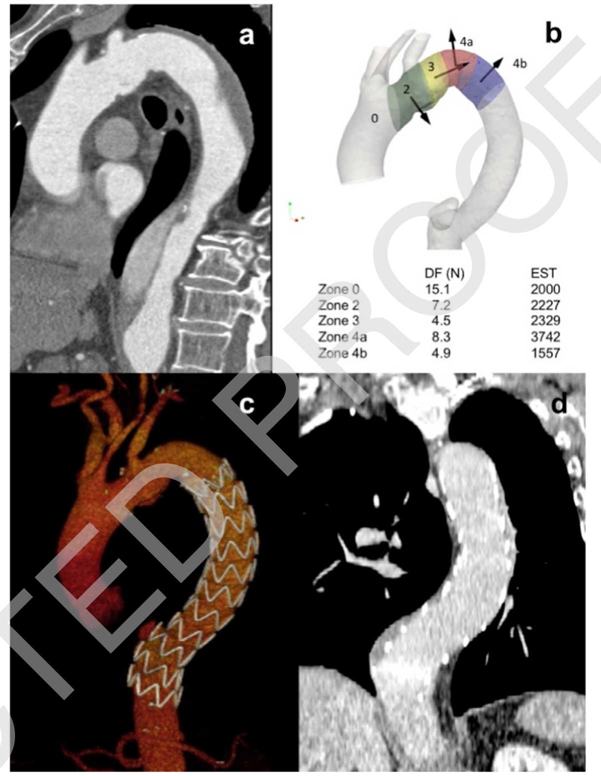

Fig. 6. (A) Preoperative Multiplanar Reconstruction (MPR) of an acute aortic type B dissection extended from the left subclavian artery to the celiac trunk. The proximal entry tear was located at the supravisceral aorta and retrograde dissection extended up to the origin of left subclavian artery.; (B) Preoperative CFD analysis conducted for EST evaluation showed higher values in zone 3 and lower in zone 4; (C) Immediate postoperative 3D volumetric rendering after deployment in zone 4b of Valiant Navion endograft (Medtronic, Santa Rosa, U.S.A.); (D) MPR of the thoracic aorta at 3 months. No migration was observed during the initial follow up period according to preoperative analysis of DF.

follow-up period, although longer results are warranted.

Geometries deeply influence the hemodynamic and mechanical behavior of both the native aorta and of the endograft deployed inside it.

It is a matter of fact that complex aortic anatomies have worse long-term outcomes with greater percentages of graft migration and endoleaks. The preoperative forecast of the DF could be helpful to improve the surgical planning and the strategy to adopt on a more personalized base.

The aim of these kinds of research is addressed to transfer the results from the bench to the surgical bedside. In this pathway, all the scientists involved, whether they are engineers or surgeons, are trying to better understand the behavior of the thoracic aorta in different geometrical conditions.

The results of such studies could impact on the daily surgical practice through the choice of different or longer proximal and/or distal landing zones, different endograft lengths or, at the other extreme, leading to the abstention from endovascular treatment when hemodynamic conditions should appear hostile or be considered reduced duration expectancy.

CONCLUSION

The role of the DFs as cause of TEVAR migration is an important issue, still in the initial phase of discussion. CFD appears essential in developing knowledge, particularly when applied to complex aortic anatomies. In addition, CFD results can be used also by the manufacturers for the development and optimization of new stent-grafts that consider both complex anatomies and increased hemodynamic DFs. In this setting, the collaboration between physicians and engineers is crucial, as both parts have a primary role in understanding and describing hidden aspects involved in TEVAR procedures as a new science applied to aortic disease. Currently, there are no guidelines that describe how to plan TEVAR in patients with more tortuous aortas. However, preliminary clinical cases based on CFD results are planned and accordingly managed, and more solid data are expected in the next future.

ACKNOWLEDGMENTS

Authors would like to thank Fulvia Domanin for original drawings.

REFERENCES

1. Goodney PP, Travis L, Lucas FL, et al. Survival after open versus endovascular thoracic aortic aneurysm repair in an observational study of the Medicare population. Circulation 2011;124:2661–9.
2. Gopaldas RR, Huh J, Dao TK, et al. Superior nationwide outcomes of endovascular versus open repair for isolated descending thoracic aortic aneurysm in 11,669 patients. J Thorac Cardiovasc Surg 2010;140:1001–10.
3. Abraha I, Romagnoli C, Montedori A, et al. Thoracic stent graft versus surgery for thoracic aneurysm. Cochrane Database Syst Rev 2016;6:CD006796.
4. Fillinger MF, Greenberg RK, McKinsey JF, et al. Reporting standards for thoracic endovascular aortic repair (TEVAR). J Vasc Surg 2010;52:1022–33.
5. Geisbüsch P, Skrypnik D, Ante M, et al. Endograft migration after thoracic endovascular aortic repair. J Vasc Surg 2018;69:1387–94.
6. Parmer SS, Carpenter JP, Stavropoulos SW, et al. Endoleaks after endovascular repair of thoracic aortic aneurysms. J Vasc Surg 2006;44:447–52.
7. Makaroun MS, Dillavou ED, Wheatley G, et al. Five year results of endovascular treatment with the Gore TAG. J Vasc Surg 2008;47:912–18.
8. Morales JP, Greenberg RK, Morales CA, et al. Thoracic aortic lesions treated with the Zenith TX1 and TX2 thoracic devices: intermediate- and long-term outcomes. J Vasc Surg 2008;48:54–63.
9. Eggebrecht H, Nienaber CA, Neuhauser M, et al. Endovascular stent-graft placement in aortic dissection: A meta-analysis. Eur Heart J 2006;27:489–98.
10. Schoder M, Czerny M, Cejna M, et al. Endovascular repair of acute type b aortic dissection: long-term follow-up of true and false lumen diameter changes. Ann Thorac Surg 2007;83 1059–6.
11. Sayer D, Bratby M, Brooks M, et al. Aortic morphology following endovascular repair of acute and chronic type b aortic dissection: Implications for management. Eur J Vasc Endovasc Surg 2008;36:522–9.
12. Parsa CJ, Schroder JN, Daneshmand MA, et al. Midterm results for endovascular repair of complicated acute and chronic type b aortic dissection. Ann Thorac Surg 2010;89:97–102.
13. Kang WC, Greenberg RK, Mastracci TM, et al. Endovascular repair of complicated chronic distal aortic dissections: intermediate outcomes and complications. J Thorac Cardiovasc Surg 2011;142:1074–83.
14. Lee CJ, Rodriguez HE, Kibbe MR, et al. Secondary interventions after elective thoracic endovascular aortic repair for degenerative aneurysms. J Vasc Surg 2013;57:1269–74.
15. Leurs LJ, Harris PL, Buth J. Secondary interventions after elective endovascular repair of degenerative thoracic aortic aneurysms: results of the european collaborators registry (eurostar). J Vasc Interv Radiol 2007;18:491–5.
16. Scali ST, Beck AW, Butler K, et al. Pathology specific secondary aortic interventions after thoracic endovascular aortic repair. J Vasc Surg 2014;59:599–607.
17. Canaud L, Marty-Ane C, Ziza V, et al. Minimum 10-year follow-up of endovascular repair for acute traumatic transection of the thoracic aorta. J Thorac Cardiovasc Surg 2015;149:825–9.
18. Ganapathi AM, Andersen ND, Hanna JM, et al. Comparison of attachment site endoleak rates in Dacron versus native aorta landing zones after thoracic endovascular aortic repair. J Vasc Surg 2014;59:921–9.
19. Kleinstreuer C, Li Z, Basciano CA, et al. Computational mechanics of Nitinol stent grafts. J Biomech 2008;41:2370–8.
20. Piccinelli M, Vergara C, Antiga L, et al. Impact of hemodynamics on lumen boundary displacements in abdominal aortic aneurysms by means of dynamic computed tomography and computational fluid dynamics. Biomech Model Mechanobiol 2013;12:1263–76.
21. Marrocco-Trischitta MM, de Beaufort HW, Secchi F, et al. A geometrical reappraisal of proximal landing zones for thoracic endovascular aortic repair according to aortic arch types. J Vasc Surg 2017;65:1584–90.
22. Marrocco-Trischitta MM, van Bakel TM, Romarowski RM, et al. The Modified Arch Landing Areas Nomenclature (MALAN) improves prediction of stent graft drag forces: proof of concept by computational fluid dynamics modelling. Eur J Vasc Endovasc Surg 2018;55:584–92.
23. Domanin M, Buora A, Scardulla F, et al. Computational fluid-dynamic analysis after carotid endarterectomy: patch graft versus direct suture closure. Ann Vasc Surg 2017;44:325–35.
24. Domanin M, Bissacco D, Le Van D, et al. Computational fluid dynamic comparison between patch-based and primary closure techniques after carotid endarterectomy. J Vasc Surg 2018;67:887–97.
25. Baethge C, Goldbeck-Wood S, Mertens S. SANRA-a scale for the quality assessment of narrative review articles. Res Integr Peer Rev. 2019;4:5.
26. SANRA checklist. https://www.aerzteblatt.de/down.asp?id=22862 [accessed 30.09.2020]
27. Green BN, Johnson CD, Adams A. Writing narrative literature reviews for peer-reviewed journals: secrets of the trade. J Chiropr Med 2006;5(3):101–17.
28. Antiga L, Piccinelli M, Botti L, et al. An image-based modeling framework for patient-specific computational hemodynamics. Med Biol Eng Comput 2008;46:1097–112.
29. Morbiducci U, Ponzini R, Rizzo G, et al. In vivo quantificationof helical blood flowin human aorta by time-resolved three-dimensional cine phase contrast magnetic resonance imaging. Ann Biomed Eng 2009;37:516–31.

30. Gallo D, De Santis G, Negri F, et al. On the use of in vivo measured flow rates as boundary conditions for image-based hemodynamic models of the human aorta: implications for indicators of abnormal flow. Ann Biomed Eng 2012;40:729–41.
31. Formaggia L, Quarteroni A, Veneziani A. Cardiovascular mathematics: modeling and simulation of the circulatory system, 1 In:. Springer Science & Business Media; 2010.
32. Les AS, Shadden SC, Figueroa CA, et al. Quantification of hemodynamics in abdominal aortic aneurysms during rest and exercise using magnetic resonance imaging and computational fluid dynamics. Ann Biomed Eng 2010;38:1288–313.
33. Passerini T, Quaini A, Villa U, et al. Validation of an open source framework for the simulation of blood flow in rigid and deformable vessels. Int J Numer Method Biomed Eng 2013;29:1192–213.
34. Taylor CA, Hughes TJR, Zarins CK. Finite element modeling of blood flow in arteries. Comput Meth Appl Mech Eng 1998;158:155–96.
35. Fung GS, Lam SK, Cheng SW, et al. On stent-graft models in thoracic aortic endovascular repair: a computational investigation of the hemodynamic factors. Comput Biol Med 2008;38:484–9.
36. Ishimaru S. Endografting of the aortic arch. J Endovasc Ther 2004;11:1162–71.
37. Altnji HE, Bou-Saïd B, Walter-Le Berre H. Morphological and stent design risk factors to prevent migration phenomena for a thoracic aneurysm: A numerical analysis. Med Eng Phys 2015;37:23–33.
38. Figueroa CA, Taylor CA, Yeh V, et al. Effect of curvature on displacement forces acting on aortic endografts: a 3-dimensional computational analysis. J Endovasc Ther 2009;16:284–94.
39. Prasad A, To LK, Gorrepati ML, et al. Computational analysis of stresses acting on intermodular junctions in thoracic aortic endografts. J Endovasc Ther 2011;18:559–68.
40. Figueroa CA, Taylor CA, Chiou AJ, et al. Magnitude and direction of pulsatile displacement forces acting on thoracic aortic endografts. J Endovasc Ther 2009;16:350–8.
41. Krsmanovic D, Koncar I, Petrovic D, et al. Computer modelling of maximal displacement forces in endoluminal thoracic aortic stent graft. Comput Methods Biomech Biomed Engin 2014;17:1012–20.
42. Nakatamari H, Ueda T, Ishioka F, et al. Discriminant analysis of native thoracic aortic curvature: risk prediction for endoleak formation after thoracic endovascular aortic repair. J Vasc Interv Radiol 2011;22:974–9.
43. Chen CK, Liang IP, Chang HT, et al. Impact on outcomes by measuring tortuosity with reporting standards for thoracic endovascular aortic repair. J Vasc Surg 2014;60:937–44.
44. Belvroy VM, Romarovski RR, Van Herwaarden JA, et al. Computational Fluid Dynamics in descending thoracic aortic aneurysm: tortuosity associated with displacement forces. J Vasc Surg 2019;69:e34.
45. Rahmani S, Grewal IS, Nabovati A, et al. Increasing angulation decreases measured aortic stent graft pullout forces. J Vasc Surg 2016;63:493–9.
46. Cheng SWK, Lam ESK, Fung GSK, et al. A computational fluid dynamic study of stent graft remodeling after endovascular repair of thoracic aortic dissections. J Vasc Surg 2008;48:303–10.
47. Fung GSK, Lam SK, Cheng SWK, et al. On stent-graft models in thoracic aortic endovascular repair: a computational investigation of the hemodynamic factors. Comp Biol Med 2008;38:484–9.
48. Wang X, Li X. Fluid-structure interaction based study on the physiological factors affecting the behaviors of stented and non-stented thoracic aortic aneurysms. J Biomech 2011;44:2177–84.
49. Grabenwöger M, Alfonso F, Bachet J, et al. Thoracic endovascular aortic repair (TEVAR) for the treatment of aortic diseases: a position statement from the European association for cardio-thoracic surgery (EACTS) and the European society of cardiology (ESC), in collaboration with the European association of percutaneous cardiovascular interventions (EAPCI). Eur Heart J 2012;33:1558–63.
50. Ueda T, Takaoka H, Raman B, et al. Impact of quantitatively determined native thoracic aortic tortuosity on endoleak development after thoracic endovascular aortic repair. AJR Am J Roentgenol 2011;197:W1140–6.
51. Madhwal S, Rajagopal V, Bhatt DL, et al. Predictors of difficult carotid stenting as determined by aortic arch angiography. J Invasive Cardiol 2008;20:200–4.
52. Melissano G, Civilini E, Bertoglio L, et al. Results of endografting of the aortic arch in different landing zones. Eur J Vasc Endovasc Surg 2007;33:561–6.